1-35 GHz MICROWAVE SCATTEROMETER

F. T. Ulaby, W. H. Stiles, D. Brunfeldt and E. Wilson
University of Kansas Center for Research, Inc.
Remote Sensing Laboratory
Lawrence, Kansas 66045

ABSTRACT

The Microwave Active Spectrometer is a truck-mounted radar capable of continuous frequency measurements over the 1-18 GHz region, and at 35.6 GHz. Its design and operational characteristics are presented, along with brief descriptions of military and civilian applications.

INTRODUCTION

Because radar is an almost all-weather sensor and time-of-day independent, the use of earth-looking imaging radar has been rapidly increasing for a variety of military applications, such as navigation and detection, and civilian applications including geologic mapping, crop classification, sea state monitoring, soil moisture monitoring and topographic mapping, among others.

The feasibility, and hence degree of success, of radar for a given application is governed by system performance and by the variability of σ^o, the backscattering coefficient. Discrimination between two neighboring targets is directly dependent on the magnitude of the difference in σ^o between the two targets. Of interest is the magnitude of the variation of σ^o between classes of targets of interest and within each class. The scattering behavior of a target, and hence the magnitude of σ^o, is governed by the target's dielectric properties and geometric configuration, with the latter measured in wavelength units. Hence, the choice of sensor parameters (frequency, polarization, and angle of incidence range) is the key to the overall radar performance for the intended application.

Recent advances in radar and associated technologies have improved system reliability and data processing capabilities, but the availability of σ^o data for various types of terrain and environmental conditions has lagged behind. To provide the needed data, a wide frequency scatterometer was designed, built, and has so far acquired over one million measurements of σ^o for a variety of targets, including bare soil, vegetation crops, trees, snow, concrete and asphalt roads, grass and vehicles.

DESIGN CONSIDERATIONS

Figure 1 shows the Microwave Active Spectrometer (MAS) in operation and Figure 2 is a close-up photograph of the antennas and RF sections of the 8-35 GHz subsystems. A summary of the system parameters is provided in Table 1. The MAS system consists of three subsystems covering the 1-8 GHz region, the 8-18 GHz region, and a single frequency channel at 35.6 GHz. Each subsystem utilizes a set of two antennas and an independent 130ns delay line used for internal calibration (signal injection). External calibration is accomplished by measuring the return power from a Luneberg lens of known radar cross-section. Block diagrams of the 8-18 GHz and 35 GHz subsystems are shown in Figure 3. The 1-8 GHz subsystem is similar to the 8-18 GHz subsystem.

Sensor Parameters

The MAS systems are capable of acquiring data at any angle between 0° (nadir) and 80°. The angle θ is controlled by an antenna positioner. Frequency coverage extends between 1 GHz and 18 GHz, plus a fixed frequency channel at 35.6 GHz. In order to simultaneously satisfy far field distance requirements and antenna beamwidth requirements, it was decided to use three sets of antennas, 4-foot and 1.5-foot diameter parabolic dishes for the 1-8 GHz and 8-18 GHz bands, respectively and lens corrected scalar horns at 35.6 GHz. In their present configuration, the MAS systems can operate in HH, HV and VV linear polarization modes at all frequencies, plus the three circular polarization modes at 35.6 GHz only. Circular polarization capability is currently being added to the 8-18 GHz band.

Measurement Accuracy

A scatterometer is a calibrated radar which provides an estimate of σ^o, the scattering coefficient (scattering cross-section per unit area) of area extensive targets by comparing the level of the power backscattered by the target to the power backscattered by a target of known radar cross-section. The accuracy, or absolute level, of such an estimate is governed by the accuracy of the measured or calculated value of the cross-section of the reference target and by the accuracy of the calibration technique.

Two types of calibration techniques are employed in the MAS system. Short-term fluctuations in the radar transfer function can be monitored by injecting the transmitter output signal into the receiver via a delay line. The delay line, which is a 100-foot coaxial cable contained in a constant temperature oven, exhibits a constant loss factor at a given microwave frequency.

Although in principle, the above internal calibration procedure in conjunction with measurements of antenna gains and cable losses, should provide the absolute measurements, the errors associated with the measurements of the antenna gains and cable losses can degrade the overall system accuracy. Hence, external calibration is used to provide end-to-end calibration. Several types of targets are usually used for calibration including flat plates, metal spheres, corner reflectors and Luneberg lenses. In choosing a calibration target suitable for field operation, the following three conditions should be satisfied: (a) known radar cross section $\sigma(m^2)$, (b) the magnitude of σ should be large enough to insure adequate target to background (clutter) ratio, and (c) broad beamwidths in the elevation and azimuth planes in order to minimize errors due to orientation misalignment. The flat plate satisfies conditions (a) and (b), but not condition (c) because its $\sigma(\theta)$ decreases rapidly with aspect angle between $\theta = 0°$ and 5°. The metal sphere can be made to satisfy all three conditions, provided its size is properly chosen. To avoid the resonance frequency region, the sphere radius should be larger than twice the signal wavelength, in which case, its radar cross section is approximately equal to its physical cross-section. At 1 GHz (λ = 30 cm), the above condition translates into a sphere diameter of the order of 1.2 m, which is difficult and expensive to construct as well as impractical to use for field operation.

Dihedral and trihedral corner reflectors are widely used to evaluate radar system performance. For accurate calibration, however, the corner reflector is judged inadequate because its radar cross-section σ exhibits a narrow beamwidth in aspect angle, typically 2° - 20°, depending on its wavelength dimensions. Among the calibration targets, the Luneberg lens has been found to be the most satisfactory for field operation. In addition to exhibiting a larger radar cross-section than a sphere and the same radar cross-section as a trihedral corner reflector (with the same physical cross-section), its backscatter beamwidth is typically 40° or larger in elevation and azimuth. At 10 GHz, for example, σ of a 9-inch diameter Luneberg lens is $15.8 m^2$, compared to $0.04 m^2$ for σ of a metal sphere of the same size, a ratio of 26 dB. The Luneberg lens is not without limitation, however. The $15.8 m^2$ value is a measured radar cross-section representing a reflector with 60% efficiency at 10 GHz, decreasing with frequency to about 10% at 18 GHz. The MAS systems use a 9-inch diameter Luneberg lens for calibration over the 1-18 GHz region and a smaller, 8-inch diameter lens, at 35.6 GHz. Each lens is mounted at the top of a 15-foot fiberglass pole covered with absorbing material. By not extending the truck boom in the external calibration mode, the antennas are at about the same height above the ground as the lens on top of the pole (30 meters away), thereby minimizing background reflections from the ground.

Measurement Resolution

In addition to accuracy, a scatterometer designer has to consider the measurement resolution (or precision) associated with the σ^o estimate. Resolution is a three-dimensional vector consisting of spectral resolution (bandwidth over which the measurement is averaged), angular resolution (determined by beamwidth, pulse-width or doppler bandwidth, depending on the system being used) and radiometric resolution (determined by the number of statistically independent samples contained in the measurement). In the general case, the product of the three resolutions is a constant. Hence improving one type of resolution results in degradation in one or both of the remaining two. Consequently, in designing a scatterometer, certain compromises have to be made within the limitations imposed by other factors such as antenna size and state-of-the-art capabilities of multi-octave microwave devices.

Angular Resolution. The resolution consideration plays an important role in the overall design of a configuration shown in Figure 4, in which $\Delta\theta$ is the angular resolution in the range direction and Δr is the range resolution. For a stationary radar, $\Delta\theta$ is the same as the antenna beamwidth β in the CW case. For a narrow pulse-width radar, $\Delta\theta$ is governed by the pulse-width, the range r and the angle of incidence θ, and for a filter limited FMCW radar, $\Delta\theta$ is governed by the IF bandwidth. From Figure 4, $\Delta\theta$ is given by the approximate expression (for $\Delta\theta << \theta$):

$$\Delta\theta = \frac{\Delta r}{r} \cot\theta \qquad (1)$$

Radiometric Resolution. If the transmitted signal is coherent in nature, the received signal is the vector sum of a large number of waves backscattered by the scatterers contained in the volume whose surface area is A. For most terrain surfaces, it is reasonable to assume that the magnitude of the electric field of the scattered waves is normally distributed and the associated phase is uniformly distributed over 2π[1]. The resultant distribution of the receiver power (and hence σ^o) is a chi-square distribution with 2N degrees of freedom, where N is the number of independent samples contained in the measurement.[1] Figure 3 shows the confidence interval associated with a measurement of σ^o, as a function of N. It is clear from Figure 5 that N must be large ($\geq$ 30) in order to have a narrow confidence interval, or equivalently an acceptable radiometric resolution. If we define the radiometric resolution ΔE as:

$$\Delta E = \left(\frac{\sigma}{\mu}\right)^2 \qquad (2)$$

where σ and μ are the standard deviation and mean of the chi-square distribution, and recognizing the right hand side of Equation (2) as 1/N for a chi-square distribution, we obtain:

$$\Delta E = \frac{1}{N} \qquad (3)$$

Frequency Resolution. Statistical independence can be achieved through spatial averaging, frequency averaging or a combination of both. If the modulation bandwidth of a stationary FMCW or chirp radar is Δf and the range resolution is Δr (Figure 4), the number of independent samples provided by frequency averaging is:

$$N_f = 2\,\frac{\Delta f}{C}\,\Delta r \qquad (4)$$

where C is the velocity of light. Alternately, the frequency resolution Δf is given by

$$\Delta f = \frac{C\,N_f}{2\Delta r} \qquad (5)$$

If measurements from N_s spatially independent cells are made and averaged, the total number of independent samples is:

$$N = N_f\,N_s \qquad (6)$$

For a single measurement ($N_s = 1$), the product of the three resolutions is obtained from Equations (1), (3) and (4):

$$\Delta\theta . \Delta E . \Delta f = \frac{c\cot\theta}{2r} \qquad (7)$$

which is a constant for fixed values of θ and r.

Choice of Parameters

To accommodate the short range requirement associated with nadir measurements (20 meters), the FMCW technique was chosen because: a) it is simple to design and construct, and b) it provides frequency averaging. In contrast, with a pulsed system, the pulse-width would have to be about 100ns or shorter and the rise and decay times about 10ns each. If FM modulation is used in the transmitter for pulse compression or frequency averaging in the receiver, the system becomes additionally more complicated, particularly if it has to operate over two or more frequency octaves.

Based on the resolution considerations discussed earlier, three sets of antennas were chosen to cover the 1-35 GHz region (Table 1), and, in order to insure that the σ^o estimate is statistically precise, spatial averaging is performed. The number of independent samples provided by frequency averaging, N_F, varies from as low as 1 sample at nadir to more than 100 samples at $\theta_o = 80°$. Hence, when the MAS system is used to acquire σ^o versus θ data, measurements are acquired from typically 30 spatially independent spots (of the distributed target under investigation) at angles close to nadir and a smaller number at large values of θ.

APPLICATION EXAMPLES

Since 1972, the MAS systems have been used to acquire data for a variety of applications. Hence, within the space limitations of this paper, only samples of results will be presented, with appropriate references provided of the more detailed reportings.

Target Descrimination

In the scan mode, the antenna beam can be made to scan in azimuth across a scene of interest at a constant angle of incidence. An example is shown in Figure 6 where the return is recorded as the beam scanned across an asphalt road with a car parked on the road. Shown are the levels of the return for grass on the two sides of the road, the asphalt (about 5 db lower), and the car. The measurements were conducted at 35 GHz with right circular polarization on both transmit and receive antennas.

The above scan was performed at $\theta = 50°$. A more complete characterization of σ^o of asphalt and grass is presented in Figures 7a and 7b respectively. Whereas the smooth surface of concrete exhibits a strong angular dependence, particularly close to nadir, grass behaves like a diffuse scattering volume.

Soil Moisture[2,3]

An experimental program was conducted to define radar parameters for sensing soil moisture content. Numerous experiments were performed to evaluate the dependence of σ^o on surface roughness, moisture content, soil type and vegetation cover. The results show that optimum operation (independence of surface roughness coupled with good vegetation penetration) is achieved in the 4-5 GHz frequency range at angles of incidence between 7° and 17° from nadir. Figure 8 shows the response of σ^o to soil moisture content, expressed in percent of field capacity.

Vegetation[4-7]

In addition to monitoring the temporal variation of σ^o of individual crops and developing models to relate σ^o to crop parameters, studies were performed to evaluate radar's capabilities as a crop classifier. An example of the temporal variation of σ^o of corn is shown in Figure 9, along with the temporal variation of the water content per unit volume of the corn canopy, expressed in logarithmic scale.

Snow[8,9]

The angular dependence of σ^o of snow is shown in Figure 10 for wet and dry conditions, and the variation of σ^o with snow water equivalent (and hence depth) is shown in Figure 11 for dry snow.

Trees[10]

A comparison of Spring and Autumn σ^o of a forest containing deciduous trees is presented in Figure 12 where it is observed that the defoliated trees (Autumn) exhibit a σ^o smaller than the fully leaved trees (Spring) by about 6-10 dB.

CONCLUSIONS

Through the use of calibrated wide frequency scatterometers, the basic data needed to evaluate the performance of a radar system for a specific application can be performed. In addition, such data can be used in the development of theoretical models of radar backscatter from terrain.

REFERENCES

1. Bush, T.F. and F. T. Ulaby, "Fading Characteristics of Panchromatic Radar Backscatter from Selected Agricultural Targets," *IEEE Transactions on Geoscience Electronics, v. GE-13, n. 4, pp. 149-157, October, 1975.*

2. Ulaby, F. T., P. P. Batlivala and M. C. Dobson, "Microwave Backscatter Dependence on Surface Roughness, Soil Moisture and Soil Texture, Part I: Bare Soil," *IEEE Transactions on Geoscience Electronics, v. GE-16, n. 4, pp. 286-295, October, 1978.*

3. Ulaby, F. T., G. A. Bradley, and M. C. Dobson, "Microwave Backscatter Dependence on Surface Roughness, Soil Moisture and Soil Texture, Part II: Vegetation-Covered Soil," *Submitted to IEEE Transactions on Geoscience Electronics, October, 1978.*

4. Ulaby, F. T. and T. F. Bush, "Monitoring Wheat Growth with Radar," *Photogrammetric Engineering and Remote Sensing, v. 42, n. 4, pp. 557-568, April, 1976.*

5. Ulaby, F. T. and T. F. Bush, "Corn Growth as Monitored by Radar," *IEEE Transactions on Antennas and Propagation, v. AP-24, n. 6, pp. 819-828, November, 1976.*

6. Attema, E. P. W. and F. T. Ulaby, "Vegetation Modeled as a Water Cloud," *Radio Science, Vol. 13, No. 2, pp. 357-364, March-April, 1978.*

7. Bush, T. F. and F. T. Ulaby, "An Evaluation of Radar as a Crop Classifier," *Remote Sensing of Environment, vol. 7, pp. 15-36, 1978.*

8. Stiles, William H. and Fawwaz T. Ulaby, "The Active and Passive Microwave Response to Snow Parameters, Part I: Wetness," *Submitted to Journal of Geophysical Research, January, 1979.*

9. Ulaby, Fawwaz T. and William H. Stiles, "The Active and Passive Microwave Response to Snow Parameters, Part II: Water Equivalent of Dry Snow," *Submitted to Journal of Geophysical Research, January, 1979.*

10. Bush, T., F. Ulaby, T. Metzler and H. Stiles, "Seasonal Variations of the Microwave Scattering Properties of Deciduous Trees As Measured in the 1-18 GHz Spectral Range," *RSL Technical Report 177-60, University of Kansas Center for Research, Inc., Lawrence, Kansas 66045, June, 1976.*

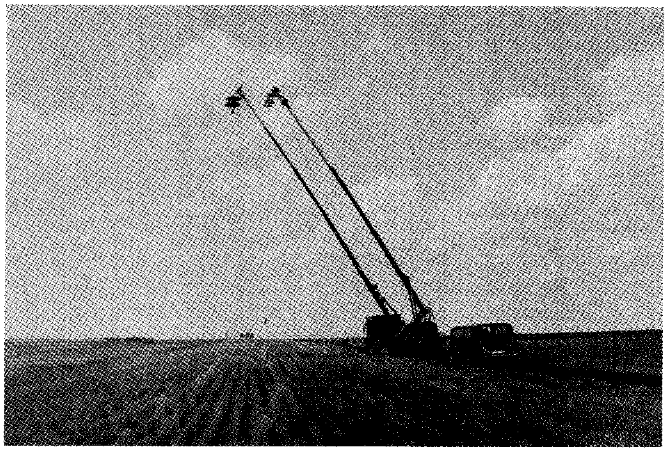

Figure 1 MAS systems acquiring data on wheat stubble. The MAS 1-8 is in the background and has the larger antennas.

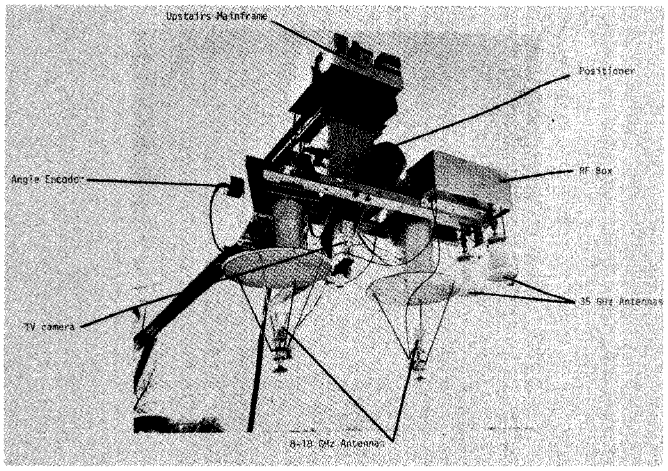

Figure 2 Upstairs Section of the MAS 8-18/35 System.

TABLE 1.

MAS 1-8 and MAS 8-18/35 Nominal System Specifications

	MAS 1-8	MAS 8-18	35 GHz Channel
Type	FM-CW	FM-CW	FM-CW
Modulating Waveform	Triangular	Triangular	Triangular
Frequency Range	1-8 GHz	8-18 GHz	35.6 GHz
FM Sweep: Δf	250 MHz	800 MHz	800 MHz
Transmitter Power	10 dBm	10 dBm	1 dBm
Intermediate Frequency	50 KHz	50 KHz	50 KHz
IF Bandwidth	10 or 20 KHz	10 KHz	10 KHz
Antennas:			
Height of Ground	26 m	23 m	23 m
Type	122 cm Reflector	46 cm Reflector	Scalar Horn
Feeds	Crossed Log-Periodic	Quad-Ridged Horn	----
Polarization Capabilities	HH, HV, VV	HH, HV, VV	HH, HV, VV, RR, RL, LL
Beamwidth	12° at 1.25 GHz to 1.8° at 7.25 GHz	4° at 8.6 GHz to 2° at 17.0 GHz	3°
Incidence Angle Range	0° (nadir)-80°	0° (nadir)-80°	0° (nadir)-80°
Calibration:			
Internal	Signal Injection (delay line)	Signal Injection (delay line)	Signal Injection (delay line)
External	Luneberg Lens Reflector	Luneberg Lens Reflector	Luneberg Lens Reflector

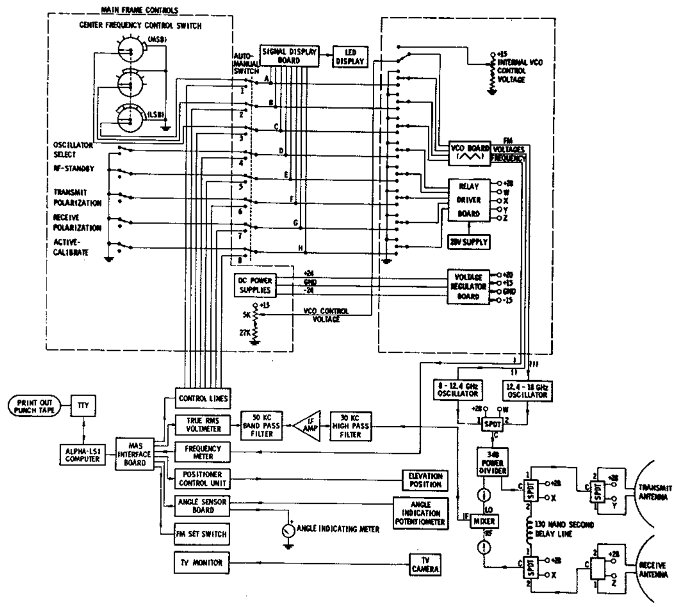

Figure 3a MAS 8-18 block diagram.

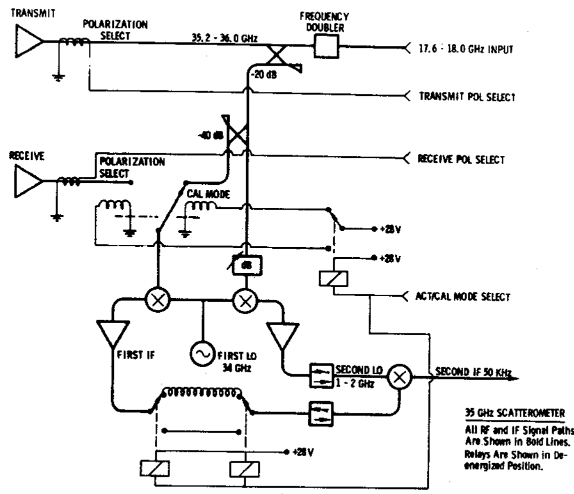

Figure 3b Overall Schematic of the 35 GHz Radar Module

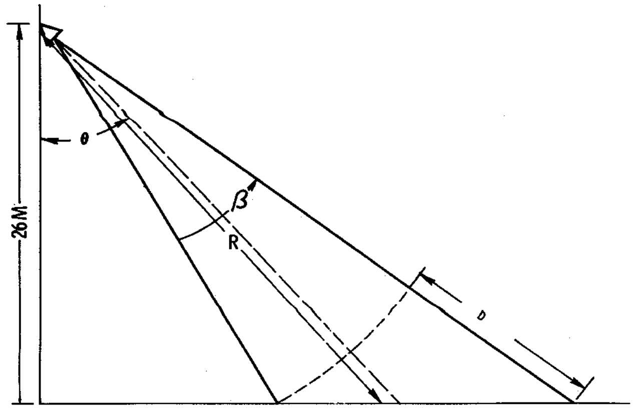

Figure 4 Illustration defining Δr: the range resolution associated with the antenna beam.

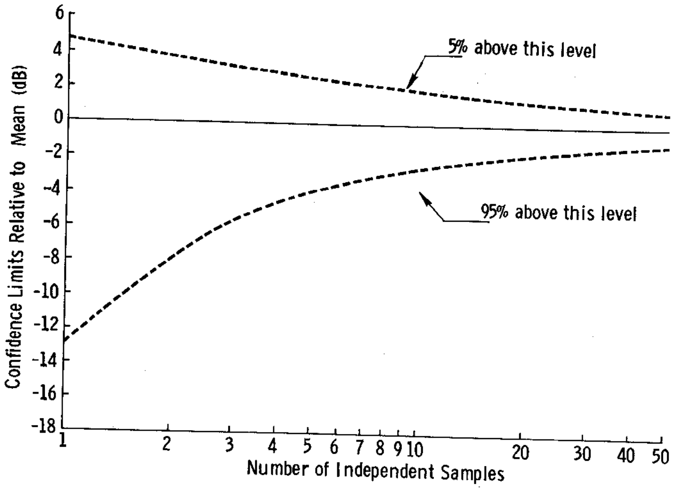

Figure 5 90 per cent confidence interval for Rayleigh distribution.

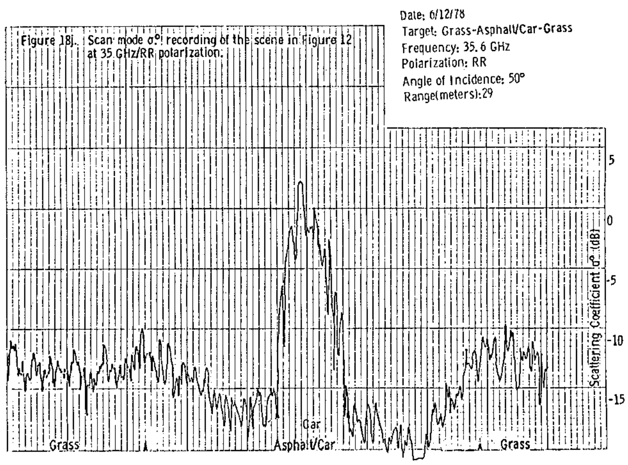

Figure 6 Scan mode σ_i^o recording the scene at 35 GHz/RR polarization.

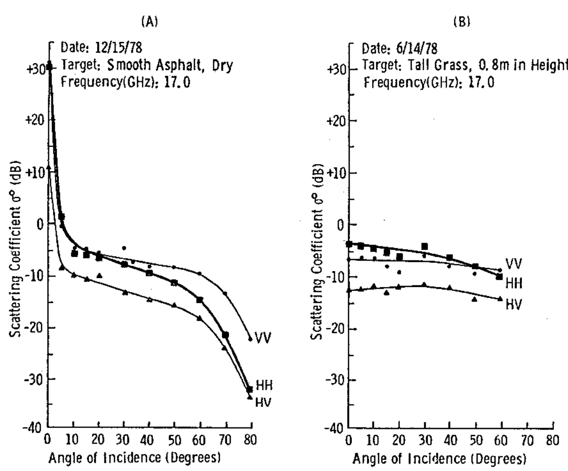

Figure 7 Angular Response for (A) Smooth Asphalt, (B) Tall Grass

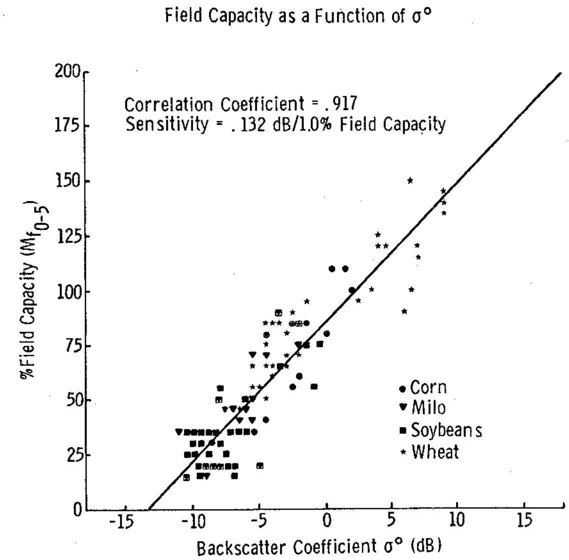

Figure 8 Percent field capacity in the 0-5 cm soil layer as a function of backscatter coefficient at 4.25 GHz, HH, 10° for corn, milo, soybean and wheat data sets combined.

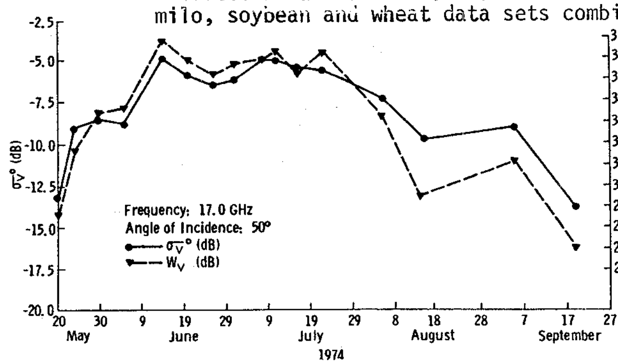

Figure 9 Temporal variations of scattering coefficient of corn σ^o(dB) (left hand scale) and the corn canopy water mass per unit volume W_v (right hand scale).

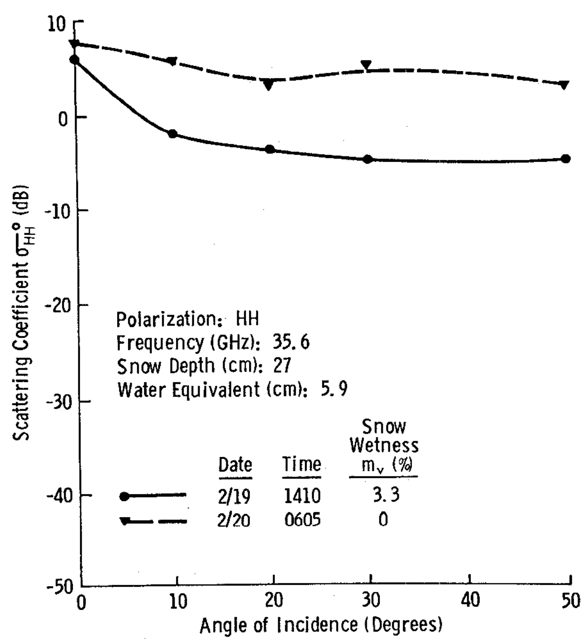

Figure 10 Angular Response of σ^o at 35.6 GHz to Wet and Dry Snow

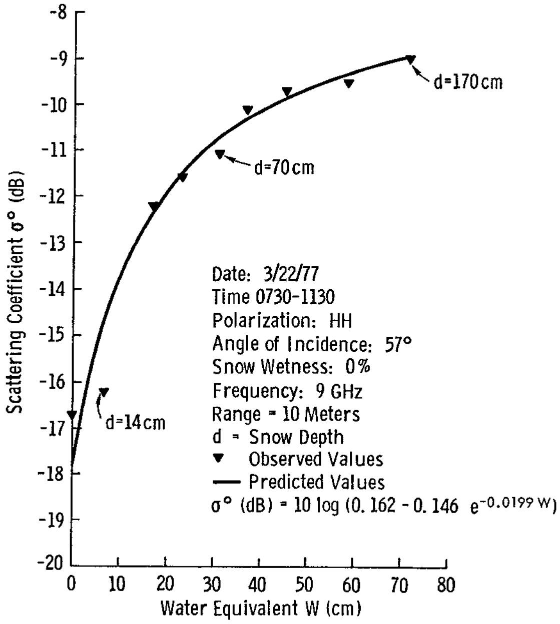

Figure 11 Scattering coefficient response to snow wetness at 9 GHz.

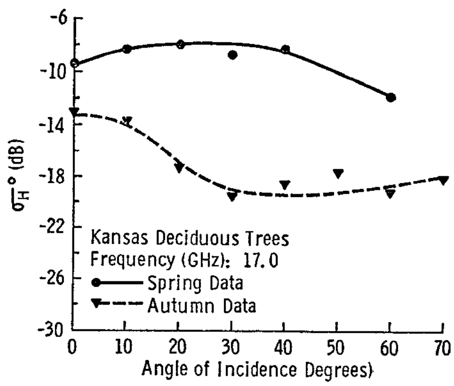

Figure 12 Angular Variations of σ_H^o of Trees Measured at 17.0 GHz in the Spring and Autumn